Published in final edited form as:
Biomacromolecules. 2012 July 9; 13(7): 2154–2162. doi:10.1021/bm300545b.

Effect of Size, Surface Charge, and Hydrophobicity of Poly(amidoamine) Dendrimers on Their Skin Penetration

Yang Yang[1], **Suhair Sunoqrot**[1], **Chelsea Stowell**[1], **Jingli Ji**[1], **Chan-Woo Lee**[2], **Jin Woong Kim**[3], **Seema A. Khan**[4], and **Seungpyo Hong**[1,*]

[1]Department of Biopharmaceutical Sciences, College of Pharmacy, University of Illinois, Chicago, IL 60612

[2]Durae Co. Research and Development Center, Gunpo, Gyeonggi-do, Republich of Korea

[3]Department of Applied Chemistry, Hanyang University, Ansan, Gyeonggi-do, Republic of Korea

[4]Robert H. Lurie Comprehensive Cancer Center, Northwestern University, Chicago, IL 60611

Abstract

The barrier functions of the stratum corneum (SC) and the epidermal layers present a tremendous challenge in achieving effective transdermal delivery of drug molecules. Although a few reports have shown that poly(amidoamine) (PAMAM) dendrimers are effective skin penetration enhancers, little is known regarding the fundamental mechanisms behind the dendrimer-skin interactions. In this paper, we have performed a systematic study to better elucidate how dendrimers interact with skin layers depending on their size and surface groups. Franz diffusion cells and confocal microscopy were employed to observe dendrimer interactions with full-thickness porcine skin samples. We have found that smaller PAMAM dendrimers (generation 2 (G2)) penetrate the skin layers more efficiently than the larger ones (G4). We have also found that G2 PAMAM dendrimers that are surface modified by either acetylation or carboxylation exhibit increased skin permeation and likely diffuse through an extracellular pathway. In contrast, amine-terminated dendrimers show enhanced cell internalization and skin retention but reduced skin permeation. In addition, conjugation of oleic acid (OA) to G2 dendrimers increases their 1-octanol/PBS partition coefficient, resulting in increased skin absorption and retention. Here we report that size, surface charge, and hydrophobicity directly dictate the permeation route and efficiency of dendrimer translocation across the skin layers, providing a design guideline for engineering PAMAM dendrimers as a potential transdermal delivery vector.

Keywords

PAMAM dendrimer; transdermal delivery; surface modification; oleic acid; partition coefficient

INTRODUCTION

The outermost layer of the skin – the stratum corneum (SC) consisting of multiple lipid layers - functions as a protective barrier against exogenous molecules.[1] In particular, the SC layers are excellent barriers against those molecules with molecular weights over 500 g/mol

*All correspondence should be addressed to: Prof. Seungpyo Hong, Ph.D., Department of Biopharmaceutical Sciences, College of Pharmacy, The University of Illinois at Chicago, 833 S. Wood St. Rm 335, Chicago, IL 60612 .

Supporting information. UV/Vis spectra for G2-RITC-NH_2, and G4-RITC-NH_2. ^{1}H NMR spectra for G2-NH_2, G4-NH_2, G2-RITC-NH_2, G2-RITC-Ac, G2-RITC-COOH, G2-RITC-NH_2-$OA_{2.3}$, and G2-RITC-NH_2-$OA_{2.7}$. This information is available free of charge via the Internet at http://pubs.acs.org.

and those with 1-octanol/PBS partition coefficients (log *P*) less than 1 or greater than 3.[2-4] For this reason, a variety of molecules and materials have been investigated as candidates that enable or facilitate skin permeation of those molecules that are otherwise skin-impermeable. Chemical penetration enhancers (CPE) have been widely used to increase the skin permeability of many therapeutic molecules and anesthetics[2]. However, the penetration-enhancing effect is frequently accompanied by skin irritation and toxicity.[2, 5] By way of contrast, polymer-based permeation enhancers typically do not cause skin irritation, but their large size often prohibits them from penetrating deep into the skin layers, which limits their efficacy.[6]

Dendrimers are synthetic, spherical macromolecules with tree-like branched structures (Figure 1 and S1). Their well-controlled sizes (3-10 nm), ease of functionalization, high water solubility, well-defined chemical structure, and biocompatibility make these nanomaterials attractive for a wide spectrum of promising biomedical applications.[7-9] Poly(amidoamine) (PAMAM) dendrimers have been shown to be advantageous over linear polymers due to their multivalency, which can be precisely controlled by engineering their surface functional groups.[7, 10] Previously, Hong et al. reported a series of studies on the biological interactions between dendrimers and either lipid bilayers or cell membranes. The studies revealed that positively charged PAMAM dendrimers induce nano-scale hole formation (within non-cytotoxic concentrations), whereas neutral or negatively charged PAMAM dendrimers do not.[11-13] These observations suggested an alternative mechanism of lipid layer permeabilization by positively charged dendrimers, which may be applicable for skin penetration.

A few recent studies have reported that, through emulsion or pretreatment, PAMAM dendrimers enhance, by as much as four-fold, the skin permeability of the nonsteroidal anti-inflammatory drugs (NSAIDs) ketoprofen and diflunisal[14] and the hydrophilic 5-fluorouracil (5FU).[15] It was also reported that permeation of 5FU was enhanced in skin pretreated with generation 4 (G4) or G3.5 PAMAM dendrimers with different surface functional groups; the order of enhancement in drug permeability coefficient (K_p) was G4-NH_2 > G4-OH > G3.5-COOH.[16] Meanwhile, the K_p of 5FU was inversely proportional to the molecular weight of the dendrimer,[15] suggesting that amine-terminated, small PAMAM dendrimers are more effective than other types of dendrimers in enhancing skin permeability of small drug molecules. However, although quite a few reports have shown enhanced skin permeation of small drug molecules mediated by PAMAM dendrimers,[14, 15, 17, 18] all of those studies used dendrimer-drug complexes to increase drug solubility and loading. Furthermore, the reported skin permeation was frequently assisted by addition of CPEs such as mineral oil and isopropyl myristate[15] or by formulating the complex into emulsions using cetyl alcohol and Brij or polysorbate as emulsifiers.[17, 19] More importantly, most of those reports have focused on skin permeation of small molecules, without providing systematic investigations focusing on the interactions of the dendrimers themselves (low-generations in particular) with the skin layers. Further mechanistic studies of how low-generation dendrimers interact with the skin layers are therefore required for better understanding and potential clinical translation of dendrimer-based transdermal drug delivery.

The primary objective of this study was to investigate the effects of dendrimer size, surface charge, and hydrophobicity as potential key parameters that determine the skin permeation/penetration behavior of dendrimers. The size effect was investigated by comparing G2 and G4 PAMAM dendrimers. The surfaces of G2 PAMAM dendrimers were then modified to be amine-, acetyl-, and carboxyl-terminated to investigate the charge effects (the chemical structures are shown in Figure 1). In addition, G2 PAMAM dendrimers were conjugated with oleic acid (OA) to control the hydrophobicities of the nanomaterials. Using those materials, we performed Franz diffusion cell experiments, confocal microscopy

observations, and partition coefficient analysis to assess the dendrimer-skin interactions. This study presents a systematic understanding of the interaction between the skin layers and surface-engineered dendrimers, demonstrating the potential of the dendrimers as a transdermal drug delivery vehicle.

EXPERIMENTAL

Materials

PAMAM dendrimers, generations 2 (G2, MW 3,256 g/mol) and 4 (G4, MW 14,215 g/mol), with ethylenediamine cores were purchased from Sigma-Aldrich (St. Louis, MO). Rhodamine B isothiocyanate (RITC), acetic anhydride, triethylamine (TEA), succinic anhydride, oleic acid (OA), *N*-(3-dimethylaminopropyl)-*N*′-ethylcarbodiimide hydrochloride (EDC), *N*-hydroxysuccinimide (NHS), anhydrous methanol, ethanol, dimethyl sulfoxide (DMSO), and 1-octanol were all obtained from Sigma-Aldrich (St. Louis, MO). Calcium- and magnesium-free PBS was purchased from Mediatech, Inc. (Manassas, VA). Polyethylene glycol 400 (PEG400) was obtained from Fisher Scientific, (Fair Lawn, NJ). All other chemicals used in this study were obtained from Sigma-Aldrich and used as received unless otherwise noted.

Synthesis and characterization of G2- and G4-RITC-NH_2 conjugates

The reaction scheme for conjugation between G2 and G4 PAMAM dendrimers and RITC is illustrated in Figure 2A. The reactions were carried out following previous reports.[17, 20] Briefly, G2 and G4 PAMAM dendrimers (10.0 mg, 3.1 Gmol and 0.7 Gmol, respectively) were dissolved in 1 mL DMSO. RITC (2.5 mg, 4.6 Gmol and 0.6 mg, 1.1 Gmol, 50% molar excess to G2 and G4, respectively) was first dissolved in 200 GL DMSO and then added to the dendrimer solutions dropwise under vigorous stirring at RT for 24 h, resulting in G2-RITC-NH_2 and G4-RITC-NH_2, respectively. Unreacted RITC was removed by membrane dialysis (Spectra/Por dialysis membrane, MWCO of 500 for G2 and 1,000 for G4, Spectrum Laboratories Inc., Rancho Dominguez, CA) in 4 L double deionized water (ddH_2O) for 3 days. The purified products were then lyophilized for 2 days and stored at −20°C. The chemical structure of the conjugates was confirmed by ^{1}H NMR in D_2O using a 400 MHz Bruker DPX-400 spectrometer (Bruker BioSpin Corp., Billerica, MA).[21] The numbers of the RITC molecules per dendrimer were calculated from UV/Vis measurements. Serially diluted RITC (1.3, 2.5, 5.0, 10.0 Gg/mL) solutions in 1:1 DMSO/H_2O were prepared and used to plot the standard curve for the quantification of the number of RITC attached to the dendrimer conjugates using a DU800 UV/Vis spectrophotometer (Beckman Coulter, CA) (Figures S2).[22] The surface charges (zeta potential, mV) of G2-RITC-NH_2 and G4-RITC-NH_2 were obtained from three repeat measurements of the aqueous dendrimer solutions at a concentration of 125 Gg/mL by quasi-elastic laser light scattering using a Nicomp 380 Zeta Potential/Particle Sizer (Particle Sizing Systems, Santa Barbara, CA) as we previously reported.[21, 22]

Preparation and chacterization of acetylated and carboxylated G2-RITC conjugates

G2-RITC-NH_2 was fully acetylated or carboxylated as previously described.[11,13] Briefly, G2-RITC-NH_2 (10.0 mg, 2.6 GmoL) was dissolved in 1 mL of methanol and acetylated by adding acetic anhydride (6.1 mg, 5.6 GL, 59.3 GmoL, 50% molar excess of the number of amines on the surface of G2-RITC-NH_2) and TEA (6.7 mg, 9.2 GL, 65.2 GmoL, 10% molar excess of acetic anhydride), under vigorous stirring at RT for 24 h (Figure 2A). In a separate reaction, G2-RITC-NH_2 (10.0 mg, 2.6 GmoL) in 1 mL of DMSO was fully carboxylated by adding succinic anhydride (5.9 mg, 59.3 GmoL, 50% molar excess of the number of amines on the surface of G2-RITC-NH_2) in 1 mL of DMSO under vigorous stirring at RT for 24 h (Figure 2A). The acetylation and carboxylation reactions were confirmed using ^{1}H NMR

measurements (Figure S3). The surface charges (zeta potential, mV) of G2-RITC-Ac, G2-RITC-COOH, and G2-RITC-NH_2 were also obtained using the same method as decribed above.

Preparation and charactierzation of G2-RITC-NH_2-OA conjugates

G2-RITC-NH_2 was reacted with OA at either 5 or 8 molar excess to G2-RITC-NH_2 using EDC/NHS chemistry (Figure 2B). For the stoichiometry of 1:5 of G2-RITC-NH_2:OA, OA (4.2 GL, 13.2 Gmol) was pre-activated by EDC (25.3 mg, 132.0 Gmol) and NHS (15.2 mg, 131.9 Gmol) in DMSO with vigorous stirring in the dark at RT for 2 h. G2-RITC-NH_2 (10.0 mg, 2.6 Gmol) in DMSO was then added and vigorously stirred for 24 h. For the 1:8 ratio, proportionally higher amounts of OA, EDC, and NHS were used under the identical conditions. Unreacted OA was removed by membrane dialysis against ddH_2O using a 500 MWCO membrane (Spectrum Laboratories) for 2 days, followed by lyophilization for 2 days and storage at −20°C. ^1H NMR and mass spectroscopy (MS, Applied Biosystems Voyager-DE Pro matrix assisted laser desorption ionization-time of flight (MALDI-TOF) mass spectrometer, Carlsbad, CA) were performed to characterize the molecular weights of the dendrimer-OA conjugates as described previously.[21, 23]

Porcine skin preparation

Full-thickness porcine skin was collected from the inner thigh area of a 30 lb female American Yorkshire pig (Halsted Packing House, Chicago, IL). The skin samples were collected from the thigh regions as these areas have generally less hair and fat compared to other regions such as dorsal, flank, and belly, to minimize the hair and fat removal process that may cause skin damage. All hairs were removed using small tweezers, and the skin was carefully examined for any defects. Undamaged skin was cut into 10 × 10 cm^2 squares with similar numbers of hair follicles. The fat and subcutaneous tissues were gently removed using a surgical blade.[15] Each piece of skin was wrapped with aluminum foil, sealed in a zip bag, stored at −80°C, and used within 90 days.[24]

Skin permeation tests using Franz diffusion cells

The porcine skin was thawed on ice, further trimmed into 1.2 × 1.2 cm^2 squares, and sandwiched between the donor and receiver chambers of the Franz diffusion cells (Φ7 mm with 0.38 cm^2 exposure area, PermeGear Inc., Hellertown, PA) with the SC side facing upward, following a previous report.[25] The receiver chambers were then filled with fresh PBS (pH 7.4). After equilibration of the skin at 37°C for 30 min, 100 GL of each dendrimer conjugate at a concentration of 1 mM or control groups (free rhodamine or vehicle (ddH_2O)) were applied to each donor chamber, as described elsewhere.[15] Note that for the dendrimer-OA conjugates, 70-ethanol solution was used as a solvent vehicle due to their poor water solubility. The chambers were first covered by Parafilm™ to prevent evaporation and then by aluminum foil to minimize fast photobleaching of rhodamine. The first sampling (t=0) was done by withdrawing 250 GL of receiver solution from each sampling portal, followed by addition of 250 GL of fresh PBS to maintain a constant total volume in the receiver chamber. Samplings were performed as frequently as every two hours up to 24 h. All sample solutions were kept at 4°C in dark before subsequent analysis.

Measurements of skin permeation and retention

The fluorescence intensity from each receiver solution was detected using a SpectraMAX GeminiXS microplate spectrofluorometer (Molecular Devices Inc., Sunnyvale, CA). The dendrimer-RITC conjugates were detected at 555 nm excitation and 590 nm emission wavelengths. The amount of dendrimer in the receiver solutions was quantified based on standard curves of fluorescence intensities versus concentrations of serially diluted solutions

from the 1 mM stock solutions of the various dendrimer conjugates (Table 1). The percent permeation (%Permeation) was calculated by dividing the amount of the conjugates in the receiver solution by the original amount applied. The materials absorbed to the epidermis and dermal layers were directly measured by extracting the conjugates from the each skin layer using a cocktail of 1:1:1 ddH_2O:ethanol:PEG400 for 6 h. In some experiments, skin absorption was also measured by subtracting the amount of the materials in the donor and receiver solutions from the total amount of the materials applied.

To confirm that the skin used was intact, we performed two observations of each square of skin before accepting the data it generated. Firstly, as the dendrimer-RITC conjugates were red in color, we observed immediate color changes (within 1 h) in receiver solutions when damaged skin was used, and such results were excluded. Secondly, we measured the fluorescence from the receiver solutions using a fluorimeter at early time points (0, 2 and 4 h) to ensure that there was the induction period that is typical for skin permeation.[15] Early permeation was considered an indicator for skin damage.

Confocal laser scanning microscopy (CLSM) observations

For the size comparison study, porcine skin was exposed to either G2-RITC-NH_2 or G4-RITC-NH_2 for 24 h in the Franz cell setup. The skin area that was exposed to the treatment was carefully collected, rinsed twice with ddH_2O for 10 min, and immersed in 10 mL of 10% neutral buffered formalin for 24 h of fixation. The fixed skin pieces were transferred into 70% (v/v) ethanol for 24 h of dehydration, followed by an overnight treatment of 30% (w/v) sucrose solution, before being embedded into cryomolds (Tissue-Tek®, Sakura Finetek USA, Inc., Torrance, CA). Skin was cryosectioned into 10 Gm-thick slices and placed on anti-frost glass slides. After drying at RT, the slides were first stained with Wheat Germ Agglutinin-Alexa Fluor 488 conjugate (WGA-AF488, 5 Gg/mL in PBS, Invitrogen Corporation, Carlsbad, CA) for 10 min at RT. After washing off the excess WGA-AF488 with ddH_2O, skin slides were mounted with antiphotobleaching mounting media with DAPI (Vector Laboratory Inc., Burlingame, CA) and covered with glass cover slips.

For the permeation pathway study, porcine skin was cut into 5×10 mm^2 strips and embedded into cryomolds. Skin was cryosectioned into 10 Gm-thick slices and placed on anti-frost glass slides. After drying at RT, the skin strips were treated with 200 nM of G2-RITC-NH_2, G2-RITC-COOH, or G2-RITC-Ac in PBS at RT for 1 h, and the excess materials were gently washed away using ddH_2O. The slides were then fixed by 10% neutral buffered formalin for 10 min at RT and washed again with ddH_2O. The slides were stained with WGA-AF488 for 10 min at RT. After washing off the excess WGA-AF488 with ddH_2O, the skin slides were mounted with antiphotobleaching mounting media with DAPI and covered with glass cover slips.

The cross-sections of the skin layers were then visualized using a Zeiss LSM 510 Meta confocal laser scanning microscope (CLSM, Carl Zeiss, Germany). The 488 nm line of a 30 mW tunable argon laser was used for the excitation of AF488, a 1 mW HeNe at 543 nm for RITC, and a 25 mW diode UV 405 nm laser for DAPI. Emission was filtered at 505-530 nm, 565-595 nm, and 420 nm for AF488, RITC, and DAPI, respectively.

Partition coefficient measurements

The partition coefficients of the surface-modified G2-RITC and the dendrimer-OA conjugates were determined using the shake-flask method.[26] Equal volumes of spectroscopic grade 1-octanol and calcium- and magnesium-free PBS were stirred together vigorously for 24 h to mutually saturate the two phases. The phases were allowed to separate overnight before aliquots were collected. Each of the water-soluble dendrimer conjugates

(except for G2-RITC-NH_2-OA) was dissolved at a concentration of 10 GM in PBS. The G2-RITC-NH_2-OA conjugates were dissolved at 10 GM in 1-octanol. The pH of each PBS solution was adjusted to 7.4 with NaOH and/or HCl. Two milliliters of the PBS phase and 2 mL of the octanol phase were gently added to a 7 mL centrifuge tube. The tube was placed on a rocker (Fisher Scientific, Pittsburgh, PA) rotating once every 3 s for 5 min and centrifuged at 20-60 ×g for 3 min. The fluorescence of the PBS phase was read using a SpectraMAX GeminiXS microplate spectrofluorometer (Molecular Devices, LLC., Sunnyvale, CA) at 555 nm excitation and 590 nm emission wavelengths. The partition coefficient, or log *P*, was calculated as

$$\log P = \log \frac{[\text{Dendrimer in Octanol}]}{[\text{Dendrimer in PBS}]}$$

The method was validated by comparing the tested value with the literature reported values of rhodamine[26] and dendrimers.[27]

Statistical analysis

Data processing was performed using Origin 8.0. Statistical analysis was performed using SPSS 11.5 based on a one-way ANOVA at $p<0.05$.

RESULTS

Characterization of the various dendrimer conjugates

The molecular weights and numbers of the terminal groups of each dendrimer as well as the numbers of fluorophores and OA attached to each dendrimer are summarized in Table 1. The UV/Vis measurements (Figure S2A) revealed that, on average, 1.0 RITC was conjugated to each G2 and G4 dendrimer molecule, which were referred to as G2-RITC-NH_2 and G4-RITC-NH_2, respectively. The RITC conjugation was confirmed using ^{1}H NMR by observing the peak(s) from the newly formed thiourea bond at 6.96 ppm as a result of conjugation between the dendrimers and the isothiocyanates (Figure S2B). The G2-RITC-NH_2 conjugates were then surface modified by acetylation or carboxylation.[13] The degree of acetylation was measured using ^{1}H NMR shown in Figure S3A, which revealed that 94% of the primary amine groups on the G2 surfaces were converted to acetamide. The shape changes of the characteristic peaks of the dendrimers after carboxylation demonstrated that the surface modification was successful (Figure S3B).[13] The zeta potential values of the various dendrimers are also listed in Table 1. G4-RITC-NH_2 exhibited the highest positively charged moiety (+41.2 mV), and G2-RITC-NH_2, G2-RITC-Ac, and G2-RITC-COOH showed highly positive (+18.8 mV), nearly neutral (+2.7 mV), and negative (−14.5 mV) surface charges, respectively, confirming the success of the surface modifications. The reaction stoichiometry (1:5 and 1:8 of G2-RITC-NH_2:OA) resulted in two different numbers of OA molecules per dendrimer, as shown in Table 1 and Figure S4. The ^{1}H NMR and MALDI-TOF data indicated that approximately 2.3 and 2.7 OA molecules were conjugated per G2-RITC-NH_2 molecule, resulting in G2-RITC-NH_2-$OA_{2.3}$ and G2-RITC-NH_2-$OA_{2.7}$, respectively.

Effect of dendrimer sizes on skin permeation

The effect of dendrimer size was investigated by comparing G2 and G4 PAMAM dendrimers conjugated with RITC. Figure 3A-C shows the confocal images of the cross-sections of the porcine skin treated with G2-RITC-NH_2 and G4-RITC-NH_2. The images demonstrated that G4-RITC-NH_2 did not penetrate across the SC, as only a small amount of the dendrimers was retained at the outermost layer of SC (Figure 3B). On the other hand, a

significantly larger amount of G2-RITC-NH_2 was absorbed into the SC layers as well as the underlying viable epidermis (Figure 3C). G2-RITC-NH_2 also exhibited a significantly stronger fluorescence signal than that of G4-RITC-NH_2, indicating that G2 dendrimers were much more strongly absorbed into the skin layers than G4. The %permeations of dendrimers showed better permeation of G2-RITC-NH_2 than G4-RITC-NH_2 in general (*data not shown*). However, the small amount of the permeated dendrimers and the large batch-by-batch variations made accurate quantification of the amount of dendrimers in the receiver solution difficult. We therefore measured the amounts of dendrimers in the skin layers instead of measuring %permeation. To quantify the dendrimer conjugates in the skin, the skin samples were collected after the Franz cell diffusion experiments, and the conjugates were extracted using a cocktail of 1:1:1 ddH_2O:ethanol:PEG400 for 6 h.

Figure 3D demonstrates the fold increases of the skin-absorbed materials after 24 h. The epidermal absorption of G2-RITC-NH_2 was 5.8-fold higher than that of G4-RITC-NH_2 after 24 h, indicating that the G2 dendrimer penetrates more efficiently than G4. Due to the better permeation of the smaller-sized G2 dendrimers, we chose them for subsequent transdermal permeation experiments that investigate the effect of charges (surface groups) and hydrophobicity on dendrimer-skin interactions.

Effect of the surface charge of dendrimers on skin permeation and retention

To assess the permeation efficiencies of the G2-RITC conjugates with different surface functional groups, Franz diffusion cell experiments were performed using a 1 mM concentration of the materials in ddH_2O without adding any commonly used permeation enhancers. The difference in permeation was observed by analyzing RITC fluorescence in the receiver solutions (Figure 3E). Although %permeation of the dendrimer conjugates was low (less than 3%), there was an approximately four-fold increase in permeation for both G2-RITC-COOH and G2-RITC-Ac compared to G2-RITC-NH_2. These results show that G2 dendrimers with different surface functional groups behave differently in terms of skin permeation. Confocal images shown in Figure 4 visualize the interactions of the various dendrimers with the skin cells, assessed by incubation of the pre-cryosectioned skin slides with the dendrimer conjugates. For clear visualization of the dendrimers in the skin layers, we added the dendrimer conjugates after cryosectioning the skin samples. As seen from the red signals from the cytoplasm (Figure 4A), G2-RITC-NH_2 was internalized into the individual cells in both the epidermal and dermal layers. By way of contrast, neither G2-RITC-COOH nor G2-RITC-Ac interacted with the cells (Figure 4B and 4C).

Effects of dendrimer hydrophobicity on skin permeation

The hydrophobicity of the materials used is quantified by log *P*. Note that the log *P* values increase with an increase of hydrophobicity of the materials. Figure 5A shows that the log *P* values of the first three types of surface modified G2 dendrimers are all negative (-0.9 ± 0.2 for G2-RITC-NH_2, -1.0 ± 0.0 for G2-RITC-Ac, and -1.3 ± 0.4 for G2-RITC-COOH). After conjugation with OA, the partition coefficients of the dendrimer-OA conjugates changed from negative to positive (1.2 ± 0.0 for G2-RITC-NH_2-$OA_{2.3}$ and 1.4 ± 0.1 for G2-RITC-NH_2-$OA_{2.7}$). To investigate the relationship between the partition coefficient and skin permeation efficiency, the skin permeation efficiencies of the various G2 PAMAM dendrimers with differing log *P* values were compared using the Franz diffusion cells. As the amounts of dendrimers that permeated across the full skin layers were relatively negligible (less than 3%), the amount of materials remaining in the donor chambers after 24 h were recorded to estimate the amounts in the skin layers (Figure 5B). While a large portion (88.6%) of the hydrophilic G2-RITC-COOH was still dispersed in the donor solution, the OA-dendrimer conjugates tended to partition more into the skin. As more OA was conjugated, less material was detected in the donor solution (44.1% and 36.8% of the

original amounts of G2-RITC-NH_2-$OA_{2.3}$ and G2-RITC-NH_2-$OA_{2.7}$, respectively), which correlates well with the partition coefficient results and confirms that the partition coefficient is a good indicator for the skin partitioning behavior of materials. The skin absorption of the rest of the conjugates was also calculated by measuring the amounts in the donor chambers: 62.7% for G2-RITC-NH_2 and 48.0% for G2-RITC-Ac.

DISCUSSION

Although several reports have studied PAMAM dendrimers as a potential skin penetration enhancer,[15-19] the skin permeation and retention behaviors of PAMAM dendrimers themselves are largely unknown. Therefore, in this study, we wanted to reveal the role of size, surface charge, and hydrophobicity of dendrimers in the skin permeation/deposition of the materials in a systematic manner. To achieve this objective, our study progressed with validating three hypotheses: (i) smaller dendrimers penetrate better than larger ones; (ii) surface modification of G2 PAMAM dendrimers enhances or alters skin permeability; and (iii) the partition coefficient (hydrophobicity) determines the permeation efficiency of the dendrimer conjugates.

The first hypothesis was assessed by comparing the size effect of dendrimers in terms of permeation efficiency and penetration depth into the skin layers (Figure 3). It is generally known that the smaller molecules penetrate through the skin layers more efficiently than their larger counterparts.[2] However, it is difficult to compare the size effect in polymeric materials while maintaining other parameters constant due to their intrinsic heterogeneity in structure and chain length. Dendrimers offer precise control over their size, providing an excellent platform for systematic studies to investigate the effects of not only size, but other parameters as well. We therefore compared the skin permeation G2 and G4 PAMAM dendrimers conjugated with RITC to investigate the size effect. The Franz diffusion cell experiments revealed that the G2 conjugates displayed better skin permeation properties (up to 3.5% and up to 0.6% for G2 and G4 after 24 hrs, respectively, *data not shown*), which is in a good agreement with literature.[28] Furthermore, the confocal images of skin cross-section shown in Figure 3 visualize that G2 conjugates penetrate deeper into the skin layers compared to G4 PAMAM dendrimers, validating the first hypothesis. Although the dendrimer conjugates used in this study underwent an extensive purification process, it needs to be noted that the conjugates may contain a degree of larger impurities, such as dimers, which may further prevent the skin penetration of particularly larger (G4) dendrimers.

Any molecule larger than 500 g/mol is generally considered impermeable through the skin.[6] However, G2-RITC-NH_2, which has a molecular weight of as high as 5,000 g/mol, still exhibits a degree of permeability and deep penetration through the porcine skin, which implies that it utilizes an alternative mechanism of penetration. Venuganti and Perumal also found, through transepidermal water loss, skin resistance measurements, and ATR-FTIR studies, that cationic dendrimers alter the skin lipid layers. G2 PAMAM dendrimers reduced skin resistance to a greater extent than higher generations of dendrimers.[16] Moreover, a series of papers published by Hong et al. demonstrated that cationic PAMAM dendrimers, such as primary amine terminated ones, induced nano-scale holes on supported lipid bilayers.[8, 11, 12] This membrane permeabilization mechanism plays a key role in the cellular internalization of PAMAM dendrimers and other positively charged polymers that have been commonly used for non-viral cell transfection or gene delivery.[12] The reduced skin resistance and membrane permeabilization by positively charged dendrimers may explain the observed skin permeation/penetration of the materials.

Our finding from the size comparison study, i.e., G2>G4, led us to further investigate the other two hypotheses using G2 PAMAM dendrimers as basal materials. Hypothesis 2 was assessed by a series of assays including permeation tests and confocal microscopy observations on cross-sections of the porcine skin. We have found that G2-RITC-NH_2 permeated the skin less effectively than G2-RITC-COOH and G2-RITC-Ac (Figure 3E). Interestingly, when delivering 5FU through the skin pretreated with PAMAM dendrimers with different surface functional groups, it was reported that the order of enhancement in K_p of 5FU was G4-NH_2 > G4-OH > G3.5-COOH.[16] However, the permeation behaviors of surface-modified dendrimers themselves do not necessarily parallel the permeation enhancement effects for a small molecule. As previously reported, amine-terminated PAMAM dendrimers internalized into the cells non-selectively.[11] The negatively charged dendrimers, on the other hand, did not internalize or bind to the cells. Due to the concentration gradient across the skin and possibly charge repulsions between the dendrimers and the negatively charged cell membrane, it is hypothesized that they go through the skin layers through an extracellular pathway that could be faster than the transcellular pathway taken by G2-RITC-NH_2. In contrast, the surface of G2-RITC-Ac is nearly neutral. It may simply follow the concentration gradient to go through the skin layers extracellularly, which also may result in a faster penetration compared to G2-RITC-NH_2. Since the theoretical molecular weight of G2-RITC-Ac (4,398 g/mol) is smaller than G2-RITC-COOH (5,346 g/mol), and based on the conclusion from the first hypothesis, it may go through the skin layers faster than G2-RITC-COOH. Due to the small size and flexible/deformable nature of PAMAM dendrimers even after surface modification, they may go through the skin layers more easily by taking the extracellular route, which results in the higher permeation efficiencies observed with G2-RITC-COOH and G2-RITC-Ac compared to G2-RITC-NH_2.

This hypothesis was further tested by confocal microscopy observations. As shown in Figure 4A, G2-RITC-NH_2 internalized into the skin cells within 1 h. This could explain the lower skin permeation efficiency of G2-RITC-NH_2, compared to G2-RITC-COOH and G2-RITC-Ac, which did not internalize into the cells (Figure 4B and 4C). Amine-terminated dendrimers internalized into individual cells both in the epidermal and dermal layers by interactions between their positively charged termini and the negatively charged cell membranes.[11] This increased uptake leads to higher accumulation of the materials in the skin layers, which makes them potential candidates for localized treatment of skin diseases. Meanwhile, carboxylated and acetylated dendrimers appeared to penetrate the skin layers better than their amine-terminated counterparts (Figure 3E). Charge repulsions, particularly between the carboxylated dendrimers and the cell membranes, may have forced them to take an extracellular route, allowing this rapid diffusion. This result highlights the potential advantage of using the carboxylated (or acetylated) dendrimers for systemic administration of active compounds through the skin, which requires fast and deep penetration through the skin layers and access to the circulation.

The third hypothesis regarding the effect of hydrophobicity on skin permeation was tested by altering the 1-octanol-to-PBS partition coefficient (log *P*) of G2-RITC-NH_2 by conjugation with different amounts of OA. The reported partition coefficient for G2-$NH_2$is −2.0,[27] and that of OA is 7.3 at pH 7.4,[29] which indicates that the G2 PAMAM dendrimer is hydrophilic whereas OA is highly hydrophobic. Since the optimum range of log *P* for SC partitioning is 1-3,[3] neither of them is easily SC-permeable when used separately. We tested if the covalent conjugation of these molecules could significantly change their partitioning behavior, and potentially make their joint log *P* fall into the optimum range for best skin permeability. The results showed that by attaching OA, the log *P* values for the conjugate was reversed from negative to positive (Figure 5A). The transition from negative to positive

was dependent on the number of the hydrophobic molecules attached. Increasing the number of OA on the surface of G2 dendrimers increased the hydrophobicity of the final conjugates.

Hydrophobic modification of the dendrimers resulted in log *P* values (1.2 and 1.4 for G2-RITC-NH_2-$OA_{2.3}$ and G2-RITC-NH_2-$OA_{2.7}$, respectively) that theoretically permit the dendrimer conjugates to readily partition into the SC. In fact, the results from the Franz cell experiments showed significantly enhanced skin partitioning of the dendrimer-OA conjugates (Figure 5B). The increase in %permeation into the receiver solutions was marginal; however, this can be attributed to the use of pure PBS in the receiver chambers as opposed to adding ethanol as reported by others.[17, 19] Further studies need to done to confirm the upper limit of the partition coefficient that dendrimer-OA conjugates can or should not exceed. Whether the value should be less than 3 for optimal skin permeation is not yet tested in our case. A linear relationship between the partition coefficient and skin permeability might exist, which could be the subject of our future investigations.

In this study, we have demonstrated that physicochemical properties of PAMAM dendrimers directly affect the skin interactions of the macromolecules. As noted, our results provide a guideline for the future development of transdermal drug delivery systems. To summarize, amine-terminated dendrimers would be beneficial for the localized transdermal delivery given their enhanced skin deposition and retention. Acetyl- or carboxyl-terminated ones would be more effective for systemic delivery through topical administration, given their enhanced permeation. Furthermore, smaller dendrimers would exhibit enhanced skin permeation and strong dendrimer-skin interactions, particularly when their hydrophobicity is optimized through conjugation with hydrophobic molecules such as drug molecules. In addition to the potential application of the surface modified dendrimers for transdermal delivery, the modularity in surface engineering enables them to be applied for controlled intestinal absorption after oral administration[30]. The paracellular and transcellular permeation pathways, observed using Caco-2 cells,[31] well correlate to our results presented in this paper, indicating the potential of the surface-engineered dendrimers to overcome the challenge of low permeability through the intestinal barriers.

CONCLUSIONS

Collectively, the results highlighted in this study confirmed the three hypotheses and allowed us to reach three main conclusions: i) smaller dendrimers penetrate the skin better than larger ones, i.e., the skin permeation and penetration depth of G2 are superior to those of G4; ii) surface modifications of PAMAM dendrimers increase skin permeation efficiencies and dictate penetration pathways; and iii) the G2-RITC-NH_2-OA conjugates with log *P* values between 1-3, the reportedly optimal range for skin partitioning, result in enhanced skin deposition, compared to not only unmodified dendrimers but also all other G2-RITC conjugates used in this study.

Our results indicate that by adjusting the stoichiometry of the dendrimer-model drug conjugation, the partition coefficient can be manipulated, which serves well as a predictor of skin permeation of the material. After surface modification with charged moieties and adjustment of log *P* values, G2 PAMAM dendrimers could be further modified through conjugation with drug molecules, targeting moieties, and imaging probes to become multifunctional, programmed nanocarriers to achieve controlled therapeutic administration through the transdermal route.

Supplementary Material

Refer to Web version on PubMed Central for supplementary material.

Acknowledgments

This work has been partially supported by Susan G. Komen Foundation under the grant # KG100713. The authors also thank Amore-Pacific Co., Ltd. for their generous gift funds to support this research. In part, this study has been also performed under the NSF-supported REU program (grant # EEC 0754590). This work was conducted in a facility constructed with support from grant C06RR15482 from the NCRR, NIH. The authors thank Dr. Ronald Koch for the helpful discussion regarding the Franz diffusion cell experiments. Thanks are extended to Dr. Jin Woo Bae and Ryan Pearson for their help on the ^{1}H NMR measurements.

REFERENCES

1. Prausnitz MR, Mitragotri S, Langer R. Current status and future potential of transdermal drug delivery. Nat. Rev. Drug Discov. 2004; 3(2):115–124. [PubMed: 15040576]
2. Karande P, Jain A, Ergun K, Kispersky V, Mitragotri S. Design principles of chemical penetration enhancers for transdermal drug delivery. Proc. Natl. Acad. Sci. U. S. A. 2005; 102(13):4688–4693. [PubMed: 15774584]
3. Subedi RK, Oh SY, Chun MK, Choi HK. Recent advances in transdermal drug delivery. Arch. Pharm. Res. 2010; 33(3):339–351. [PubMed: 20361297]
4. Finnin BC, Morgan TM. Transdermal penetration enhancers: Applications, limitations, and potential. J. Pharm. Sci. 1999; 88(10):955–958. [PubMed: 10514338]
5. Williams AC, Barry BW. Penetration enhancers. Adv. Drug Deliv. Rev. 2004; 56(5):603–618. [PubMed: 15019749]
6. Akimoto T, Nagase Y. Novel transdermal drug penetration enhancer: synthesis and enhancing effect of alkyldisiloxane compounds containing glucopyranosyl group. J. Control. Release. 2003; 88(2): 243–252. [PubMed: 12628331]
7. Myung JH, Gajjar KA, Saric J, Eddington DT, Hong S. Dendrimer-Mediated Multivalent Binding for the Enhanced Capture of Tumor Cells. Angew. Chem. Int. Ed. Engl. 2011; 50(49):11769–72. [PubMed: 22012872]
8. Leroueil PR, Hong S, Mecke A, Baker JR Jr. Orr BG, Banaszak Holl MM. Nanoparticle interaction with biological membranes: does nanotechnology present a Janus face? Acc. Chem. Res. 2007; 40(5):335–342. [PubMed: 17474708]
9. Duncan R. Polymer conjugates as anticancer nanomedicines. Nat. Rev. Cancer. 2006; 6(9):688–701. [PubMed: 16900224]
10. Hong S, Leroueil PR, Majoros I. n. J. Orr BG, Baker JR Jr, Banaszak Holl MM. The Binding Avidity of a Nanoparticle-Based Multivalent Targeted Drug Delivery Platform. Chem. Bio. 2007; 14(1):107–115. [PubMed: 17254956]
11. Hong S, Bielinska AU, Mecke A, Keszler B, Beals JL, Shi X, Balogh L, Orr BG, Baker JR Jr. Banaszak Holl MM. Interaction of poly(amidoamine) dendrimers with supported lipid bilayers and cells: hole formation and the relation to transport. Bioconj. Chem. 2004; 15(4):774–782.
12. Hong S, Leroueil PR, Janus EK, Peters JL, Kober M-M, Islam MT, Orr BG, Baker JR Jr. Banaszak Holl MM. Interaction of polycationic polymers with supported lipid bilayers and cells: nanoscale hole formation and enhanced membrane permeability. Bioconj. Chem. 2006; 17(3):728–734.
13. Hong S, Rattan R, Majoros IJ, Mullen DG, Peters JL, Shi X, Bielinska AU, Blanco L, Orr BG, Baker JR Jr. Banaszak Holl MM. The Role of Ganglioside GM(1) in Cellular Internalization Mechanisms of Poly(amidoamine) Dendrimers. Bioconj. Chem. 2009; 20(8):1503–1513.
14. Cheng Y, Man N, Xu T, Fu R, Wang X, Wang X, Wen L. Transdermal delivery of nonsteroidal anti-inflammatory drugs mediated by polyamidoamine (PAMAM) dendrimers. J. Pharm. Sci. 2007; 96(3):595–602. [PubMed: 17094130]
15. Venuganti VVK, Perumal OP. Effect of poly(amidoamine) (PAMAM) dendrimer on skin permeation of 5-fluorouracil. Intl. J. Pharm. 2008; 361(1-2):230–238.
16. Venuganti VVK, Perumal OP. Poly(amidoamine) dendrimers as skin penetration enhancers: Influence of charge, generation, and concentration. J. Pharm. Sci. 2008; 98(1520-6017):2345–2356. [PubMed: 18937369]
17. Filipowicz A, Wolowiec S. Solubility and in vitro transdermal diffusion of riboflavin assisted by PAMAM dendrimers. Intl. J. Pharm. 2011; (408):152–156.

18. Chauhan AS, Sridevi S, Chalasani KB, Jain AK, Jain SK, Jain NK, Diwan PV. Dendrimer-mediated transdermal delivery: enhanced bioavailability of indomethacin. J. Control. Release. 2003; 90(3):335–343. [PubMed: 12880700]
19. Borowska K, Laskowska B, Magon A, Mysliwiec B, Pyda M, Wolowiec S. PAMAM dendrimers as solubilizers and hosts for 8-methoxypsoralene enabling transdermal diffusion of the guest. Intl. J. Pharm. 2010; (398):185–189.
20. Majoros IJ, Thomas TP, Mehta CB, Baker JR Jr. Poly(amidoamine) Dendrimer-Based Multifunctional Engineered Nanodevice for Cancer Therapy. J. Med. Chem. 2005; 48(19):5892–5899. [PubMed: 16161993]
21. Bae JW, Pearson RM, Patra N, Sunoqrot S, Vukovic L, Kral P, Hong S. Dendron-mediated self-assembly of highly PEGylated block copolymers: a modular nanocarrier platform. Chem. Commun. 2011; 47(37):10302–10304.
22. Sunoqrot S, Bae JW, Jin S-E, M. Pearson R, Liu Y, Hong S. Kinetically Controlled Cellular Interactions of Polymer-Polymer and Polymer-Liposome Nanohybrid Systems. Bioconj. Chem. 2011; 22(3):466–474.
23. Lalwani S, Chouai A, Perez LM, Santiago V, Shaunak S, Simanek EE. Mimicking PAMAM Dendrimers with Ampholytic, Hybrid Triazine Dendrimers: A Comparison of Dispersity and Stability. Macromolecules. 2009; 42(17):6723–3732. [PubMed: 20711424]
24. Polat BE, Seto JE, Blankschtein D, Langer R. Application of the aqueous porous pathway model to quantify the effect of sodium lauryl sulfate on ultrasound-induced skin structural perturbation. J. Pharm. Sci. 2010; 100(4):1387–1397.
25. Tong YC, Yu TY, Chang SF, Liaw JH. Nanopolymeric Micelle Effect on the Transdermal Permeability, the Bioavailability and Gene Expression of Plasmid. Mol. Pharm. 2012; 9(1):111–120. [PubMed: 22142416]
26. Dinerman AA, Cappello J, El-Sayed M, Hoag SW, Ghandehari H. Influence of Solute Charge and Hydrophobicity on Partitioning and Diffusion in a Genetically Engineered Silk-Elastin-Like Protein Polymer Hydrogel. Macromol. Biosci. 2010; 10(10):1235–1247. [PubMed: 20602417]
27. Giri J, Diallo MS, Goddard W. A. r. Dalleska NF, Fang X, Tang Y. Partitioning of Poly(amidoamine) Dendrimers between n-Octanol and Water. Environ. Sci. Technol. 2009; 43(13):5123–5129. [PubMed: 19673317]
28. Venuganti V, Sahdev P, Hildreth M, Guan X, Perumal O. Structure-Skin Permeability Relationship of Dendrimers. Pharm. Res. 2011; 28(9):2246–2260. [PubMed: 21633876]
29. Buist HE, van Burgsteden JA, Freidig AP, Maas WJM, van de Sandt JJM. New in vitro dermal absorption database and the prediction of dermal absorption under finite conditions for risk assessment purposes. Regul. Toxicol. Pharmacol. 2010; 57(2-3):200–209. [PubMed: 20178823]
30. El-Sayed M, Ginski M, Rhodes C, Ghandehari H. Transepithelial transport of poly(amidoamine) dendrimers across Caco-2 cell monolayers. J. Control. Release. 2002; 81(3):355–365. [PubMed: 12044574]
31. Lin Y-L, Khanafer K, El-Sayed MEH. Quantitative evaluation of the effect of poly(amidoamine) dendrimers on the porosity of epithelial monolayers. Nanoscale. 2010; 2(5):755–762. [PubMed: 20648321]

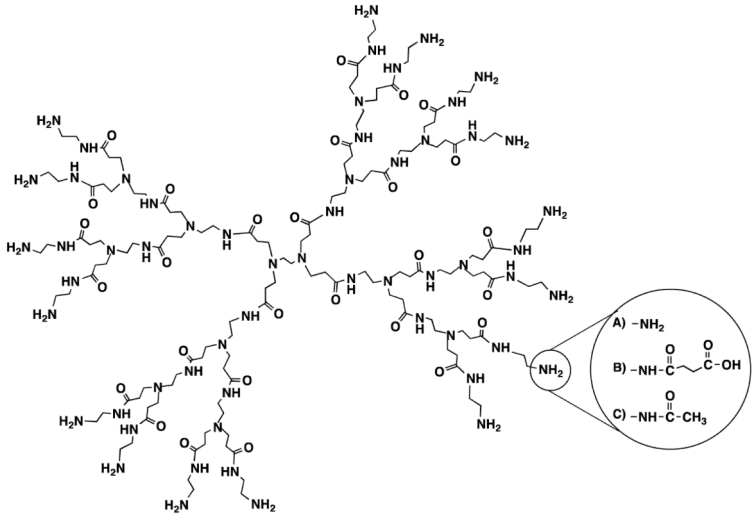

Figure 1. Chemical structure of G2 PAMAM dendrimer

The representative structure of the surface modified dendrimers: A) amine-, B) carboxyl-, and C) acetyl-terminated dendrimers.

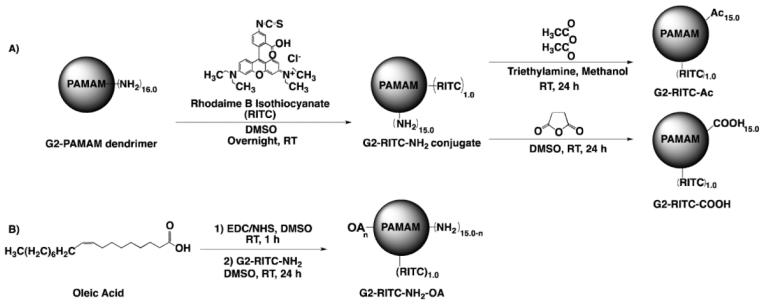

Figure 2. Reaction schemes of the surface modifications of G2 PAMAM dendrimers

A) Conjugation of G2-RITC-NH_2 (same conditions for G4-RITC-NH_2 conjugation), and surface charge modification by acetylation and carboxylation of G2-RITC-NH_2; B) conjugation of OA to G2-RITC-NH_2.

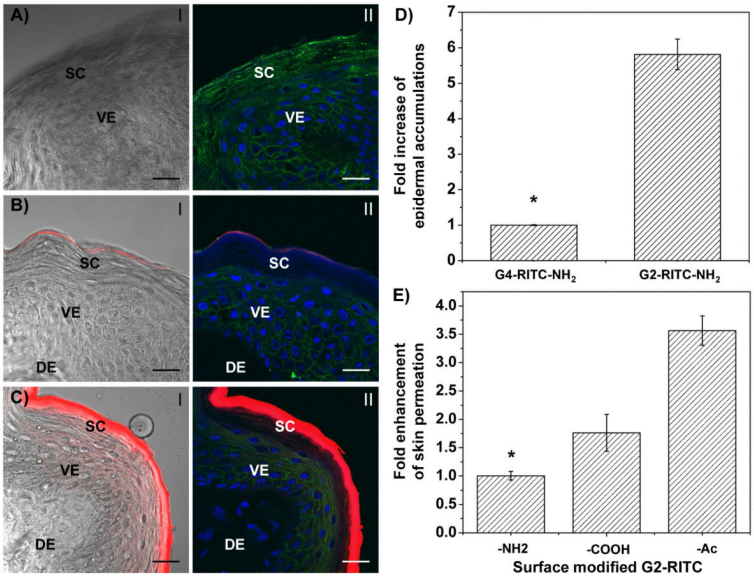

Figure 3. Skin permeation efficiencies of various PAMAM dendrimers

A<C) CLSM images of the skin cross-sections of microtomed porcine skin layers after treatment with dendrimers. A) Vehicle (ddH_2O) control, B) G4-RITC-NH_2, and C) G2-RITC-NH_2. (I, overlay of red channel (dendrimer conjugates) and bright field images; II, merged images of dendrimer conjugates (red), cell membrane stained by WGA-AF488 (green), and nuclei stained by DAPI (blue). **D)** Fold increase in epidermal accumulations of G2 and G4 PAMAM dendrimers over 24 h (error bars: standard deviation (SD), n=3). Note that the smaller molecular size leads to better skin absorption; in this case G4-RITC < G2-RITC. **E)** Fold enhancement in %permeation of the surface modified G2 PAMAM dendrimers after 24 h (error bars: SD, n=3-6). Note that the both neutral and negatively charged dendrimers permeate skin more efficiently than the positively charged dendrimers. Scale bar: 10 Gm. SC, stratum corneum; VE, viable epidermis; DE, dermal layer. *p<0.05.

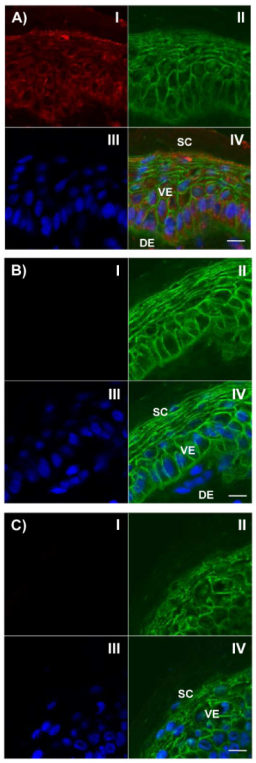

Figure 4.

Confocal images of cross-sections of microtomed porcine skin layers after 1 h treatment with: A) G2-RITC-NH_2; B) G2-RITC-COOH; or C) G2-RITC-Ac. The dendrimer conjugates (I, red); cell membranes stained by WGA-AF488 (II, green); nuclei stained by DAPI (III, blue); and merged images of all three channels (IV) are shown in each quadrant. Note that G2-RITC-NH_2 strongly interacts with the epidermal/dermal cells whereas G2-RITC-COOH and G2-RITC-Ac do not. Scale bar: 10 Gm. SC, stratum corneum; VE, viable epidermis; DE, dermal layer.

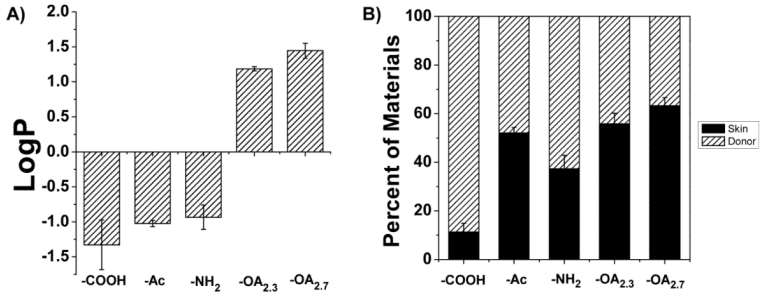

Figure 5. Relationships between hydrophobicity and skin retention of the surface modified G2 dendrimers

A) Partition coefficients of various G2 PAMAM dendrimers measured using the shake-flask method. The experimental groups include G2-RITC-COOH, G2-RITC-Ac, G2-RITC-NH_2, and two types of OA-conjugated dendrimers: G2-RITC-NH_2-$OA_{2.3}$ and G2-RITC-NH_2-$OA_{2.7}$. The observed higher skin deposition of the G2-RITC-NH_2-OA conjugates is likely a result of their higher partition coefficients than other types of dendrimers. **B)** Skin deposition and retention of various G2 PAMAM dendrimers and their conjugates after 24 h of the Franz cell experiment (error bars: standard error from the donor solution, n=3).

Table 1

Characterization of dendrimer conjugates.

	Surface NH_2 groups	Fluorophore Attached[a]	Fluorophore Attached[b]	Measured MW (Da)[c]	Theoretical MW (Da)	ζ-Potential (mV)[d]
G2-NH_2	16	0	0	3,160-3,253	3,256	+16.6
G4-NH_2	64	0	0	10,709-15,287	14,215	+38.5
G4-RITC-NH_2	63	1.0	-	9,101-19,000	15,753	+41.2
G2-RITC-NH_2	15	1.0	1.3	4,155	3,792	+18.8
G2-RITC-Ac	0	1.0	1.3	4,399	4,398	+2.7
G2-RITC-COOH	0	1.0	1.3	5,655	5,346	−14.5
G2-RITC-NH_2-$OA_{2.3}$	13	1.0	1.3	4,389	4,638	N/A[e]
G2-RITC-NH_2-$OA_{2.7}$	10	1.0	1.3	3,708-5,643	5,202	N/A[e]

[a] Measured using UV/Vis spectroscopy.

[b] Measured using ^{1}H NMR.

[c] Meausred using MALDI-TOF.

[d] Measured using Zeta Potential/Particle Sizer.

[e] Zeta potential of OA conjugates were not measured due to the limited solubility in aqueous solutions.

Biomacromolecules. Author manuscript; available in PMC 2013 July 09.